Journal of Alloys and Compounds 495 (2010) 7–12

Contents lists available at ScienceDirect

Journal of Alloys and Compounds

journal homepage: www.elsevier.com/locate/jallcom

Structural and electrical properties of $Ba_{5-x}Ca_xSmTi_3Nb_7O_{30}$ ($x = 0–5$) ferroelectric ceramics

Prasun Ganguly, A.K. Jha*

Thin Film & Materials Science Laboratory, Department of Applied Physics, Delhi Technological University (Formerly Delhi College of Engineering), Bawana Road, Delhi 110042, India

ARTICLE INFO

Article history:
Received 26 December 2009
Received in revised form 15 January 2010
Accepted 21 January 2010
Available online 2 February 2010

Keywords:
Ceramics
Ferroelectrics
Solid state reaction
Dielectric response
X-ray diffraction
Scanning electron microscopy

ABSTRACT

Samples of the compositions $Ba_{5-x}Ca_xSmTi_3Nb_7O_{30}$ ($x = 0–5$), where Ba has been replaced by Ca in steps, were synthesized by solid state reaction method and studied for their structural, dielectric and electrical properties. X-ray diffraction analysis shows the formation of the compounds in an orthorhombic structure at room temperature. Scanning electron micrographs reveal that the average grain size of the compounds increases with increase in calcium content. Detailed studies of dielectric properties as a function of temperature at different frequencies suggest that the synthesized compounds undergo non-relaxor type ferroelectric–paraelectric phase transition of diffuse nature with a decrease in the value of dielectric constant as calcium content increases. When barium is completely replaced by calcium (i.e., $Ca_5SmTi_3Nb_7O_{30}$), the compound does not show any phase transition. The ferroelectric nature of the studied compounds was confirmed by recording the polarization–electric field (P–E) hysteresis loops at room temperature. The remanent polarization value is observed to be highest in the sample with $x = 1$. The temperature variation of P–E loop in the Ca free compound has been reported. The dc and ac conductivity study over a wide temperature range suggests that the compounds have negative temperature coefficient of resistance (NTCR) behaviour.

1. Introduction

From the first report of ferroelectricity in $BaTiO_3$ [1], there has been an increasing interest in developing and searching new ferroelectric materials for device applications, which has led to the discovery of numerous ferroelectric materials. During the process, a large number of ferroelectric oxides of different structural families such as perovskite, spinel, tungsten–bronze (TB), etc., have been discovered. Some of the ferroelectric niobates of TB structure have excellent properties such as pyroelectric, electro-optic, photorefractive, piezoelectric, etc., useful for device applications [2–6]. The TB-type structure consists of a complex array of distorted BO_6 octahedral sharing corners in such a way that three different types of interstices (A, B and C) are available for cation occupation in the general formula $[(A_1)_4(A_2)_2(C)_4][(B_1)_2(B_2)_8]O_{30}$ [7] where A_1 and A_2 sites are usually filled by divalent or trivalent cations, B_1 and B_2 sites by tetravalent or pentavalent cations and C site being small, often remains empty giving the general formula $A_6B_{10}O_{30}$. There is a scope for substitution by variety of cations at many interstitial sites (i.e., A_1, A_2, B_1 and B_2) that can tailor the physical properties of the compound for various device applications. In order to find some new TB niobate ceramics, some work has been carried out in $BaO–R_2O_3–TiO_2–Nb_2O_5$ (R = rare earth) quaternary systems [8–11]. These compounds were found to be interesting because of their nature of diffuse phase transition with transition temperature well above room temperature [12]. Detailed literature survey shows that even though a lot of work has been done on the TB-compounds, not much work has been reported in the $Ba_{5-x}Ca_xRTi_3Nb_7O_{30}$ (R = rare earth); $x = 0–5$, compounds. This prompted the authors to make a detailed study of $Ba_{5-x}Ca_xSmTi_3Nb_7O_{30}$ (BCSTN) ($x = 0, 1, 2, 3, 4$ and 5) compounds and studied for their structural, dielectric, ferroelectric and electrical properties.

2. Experimental

The polycrystalline samples of BCSTN were prepared by solid state reaction technique by taking high purity $CaCO_3$, $BaCO_3$, TiO_2, Nb_2O_5 (all from M/s Aldrich, USA) and Sm_2O_3 (M/s Alfa Aesar, USA) in their stoichiometric proportions. The materials were thoroughly ground in an agate mortar and passed through sieve of extremely fine mesh size. This powder mixture was then calcined at 1100 °C for 20 h in an alumina crucible. The calcined mixture was ground, passed through the sieve again. The mixture was then admixed with 5 wt.% polyvinyl alcohol (M/s Aldrich, USA) as a binder and then pressed at ~300 MPa into disk shaped pellets. These pellets were then sintered at 1300 °C for 10 h. This sintering condition is the optimized sintering condition and the details are reported elsewhere [13].

X-ray diffractogram of the sintered pellets were recorded using Bruker diffractometer (model D8 Advance) in the range $20° \leq 2\theta \leq 70°$ with Cu Kα radiation

* Corresponding author. Tel.: +91 9868242150; fax: +91 11 27871023.
E-mail address: dr_jha_ak@yahoo.co.in (A.K. Jha).

0925-8388/$ – see front matter © 2010 Elsevier B.V. All rights reserved.
doi:10.1016/j.jallcom.2010.01.118

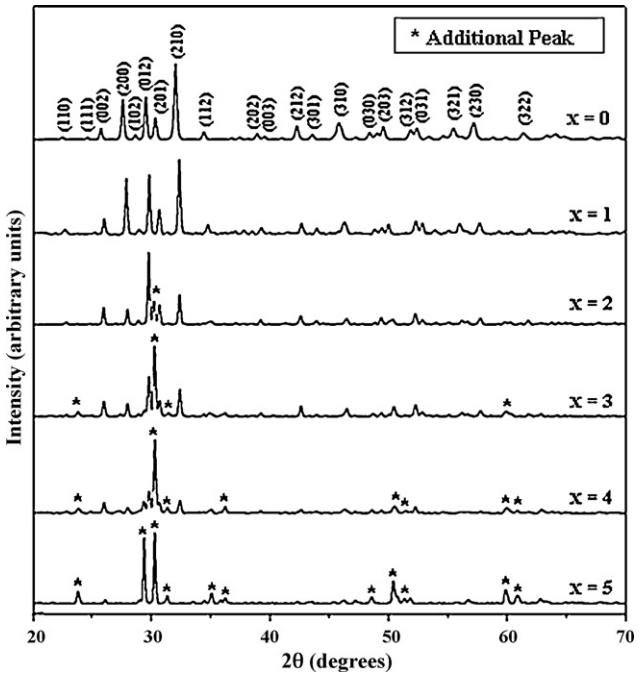

Fig. 1. X-ray diffraction patterns of $Ba_{5-x}Ca_xSmTi_3Nb_7O_{30}$ ($x = 0$–5) compounds.

($\lambda = 1.5405$ Å) with a scanning rate of 1°/min. The granular morphology of the samples was investigated using scanning electron microscope (JEOL, JSM-840), operated at 20 kV. The sintered pellets were polished and silver pasted on both sides and cured at 325 °C for 1 h. The dielectric measurements were carried out using a precision LCR meter (Agilent 4284A) operating at oscillation amplitude of 1 V. The polarization–electric field (P–E) hysteresis loops were recorded using a P–E loop tracer based on Sawyer–Tower circuit. The dc electrical resistivity of the samples was measured from room temperature to 300 °C at constant electric field (60 V/cm), using a Keithley 6517A programmable electrometer.

3. Results and discussion

3.1. XRD and SEM analysis

Fig. 1 shows the XRD patterns of the various BCSTN sintered samples. It is observed in the diffractogram that the specimen remains single phase only up to $x = 1$. For the samples with $x \geq 2$, additional peaks are also observed which indicates the formation of secondary phase. As the calcium concentration increases, the splitting as well as the intensity of additional peaks increased. A comparison of the additional peaks with standard XRD patterns (JCPDS file No. 30-0270) shows the formation of $Ca_3Nb_2Ti_3O_{14}$ as secondary phase. Lattice parameters were calculated from the X-ray diffractograms and refined using least square refinement method by a computer program package – PowderX [14] – are listed in Table 1. A decrease in the lattice constants is observed which can be understood as ionic radius of Ca^{2+} (1.00 Å) is less than that of Ba^{2+} (1.36 Å) [15]. The crystal structural distortion parameters, namely, orthorhombicity $[2(a-b)/(a+b)]$ and tetragonal strain (c/a) have been calculated and plotted as a function of calcium concentration (Fig. 2). It is observed that the tetragonality increases while orthorhombicity decreases as calcium content is increased.The SEM micrographs of the Ca free and Ca-substituted samples are shown in Fig. 3 which shows considerable increase in grain size with increasing Ca content. The average grain size in the sample with $x = 0$ is ~2 μm while in the sample with $1 \leq x \leq 5$ the size is found to be in the range of ~10–17 μm. The shape of grains changes from oval to rod like structure with increase in Ca content. Similar shape change of grains on addition of calcium has been reported earlier also [16]. However, it can be seen that the size of rod like structure reduces in barium free sample.

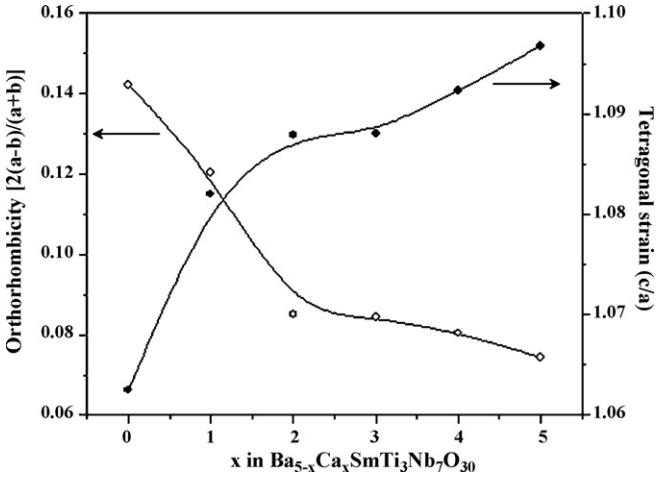

Fig. 2. Compositional variation of orthorhombicity and tetragonal strain.

3.2. Dielectric properties

Fig. 4 shows the temperature dependence of dielectric constant (ε'_r) and dielectric loss ($\tan\delta$) for all the compounds at different frequencies (1, 10 and 100 kHz). It is observed that the compounds with $x = 0$–4 undergo ferroelectric–paraelectric phase transition of diffuse type at the Curie temperature (T_c), whereas the compound with $x = 5$ does not show any dielectric anomaly in the measured temperature range. It is also observed that all the compounds have the same T_c at all the above mentioned frequencies, suggesting that the compounds do not show any relaxor behaviour. This result is somewhat different from the earlier results obtained in $Ba_5SmTi_3Nb_7O_{30}$ ceramic reported by Shannigrahi et al. [8] where the sample was sintered at 1250 °C for 24 h and the specimen shows relaxor behaviour, lower T_c, higher $\varepsilon'_{r\,max}$ values. In this class of materials, it is known that sintering process strongly influences phase constitutes, grain size, grain uniformity, internal stress, etc. [17]. Hence these differences in result may be due to the difference in sintering temperature used in both the studies. Moreover, it is known that concentration of oxygen vacancies increases with increase in sintering temperature in this compound [13] and the relaxor behaviour diminishes due to defects such as oxygen vacancy as polar clusters formed by oxygen vacancies never freezes [18]. So, in the present work, a higher sintering tem-

Table 1
Different parameters of $(Ba_{1-x}Ca_x)_5SmTi_3Nb_7O_{30}$ ($x = 0$–5) compounds.

x	a (Å)	b (Å)	c (Å)	T_c (°C)	$\varepsilon'_{r\,max}$ at 100 kHz	γ	$2P_r$ (μC/cm^2)	$2E_c$ (kV/cm)	E_a (eV)
0	6.4106	5.5595	6.8112	170	303	1.71	2.3	23.3	0.57
1	6.3078	5.5914	6.8250	198	243	1.10	2.5	36.7	1.10
2	6.2608	5.7506	6.8111	30	220	1.50	1.0	10.3	0.59
3	6.2629	5.7556	6.8139	80	147	1.52	0.8	18.4	0.40
4	6.2480	5.7650	6.8244	85	64	1.60	0.7	22.9	0.38
5	6.1924	5.7484	6.7915	–	38	–	–	–	0.45

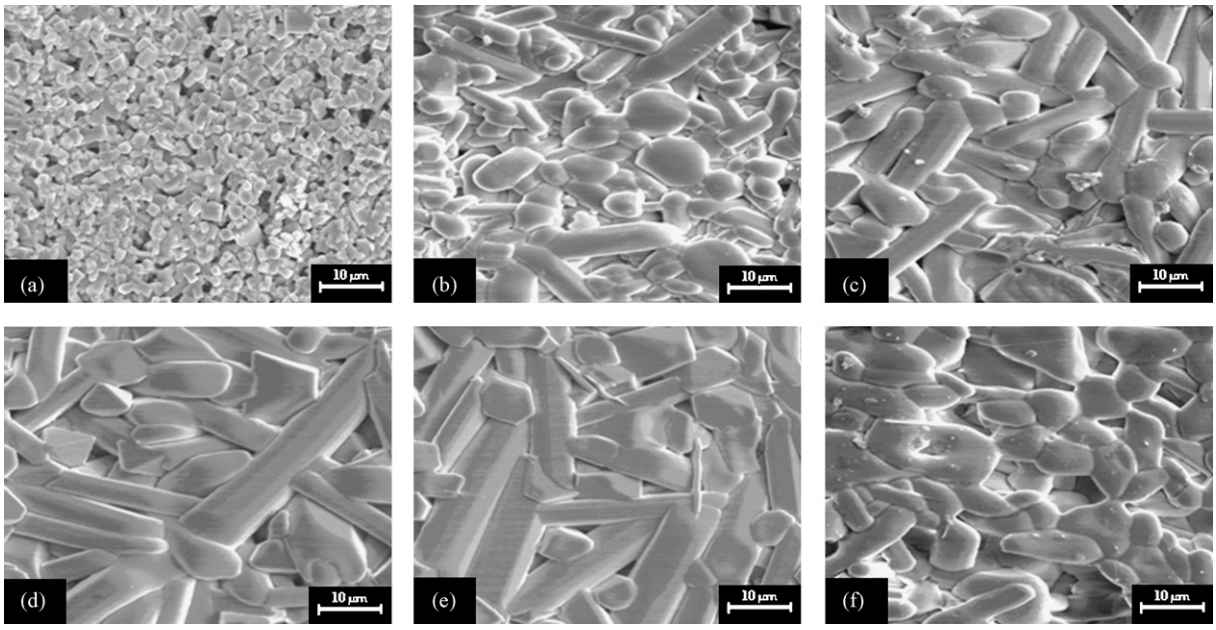

Fig. 3. SEM micrographs of $(Ba_{1-x}Ca_x)_5SmTi_3Nb_7O_{30}$ samples with (a) $x = 0$, (b) $x = 1$, (c) $x = 2$, (d) $x = 3$, (e) $x = 4$ and (f) $x = 5$.

perature (1300 °C) compared to the earlier work [8] results in an increased concentration of oxygen vacancies that possibly mask the relaxor behaviour of the compound. Further, the dielectric constant decreases as the concentration of calcium increases (Table 1). This is possibly due to the decrease in the net polarization of the compounds with increase in Ca concentration as the ionic polarizability, α_I of Ca is 3.16 Å^3 compared to that of Ba 6.40 Å^3 [19]. However, T_c increases from 170 °C (in Ca free specimen) to 198 °C

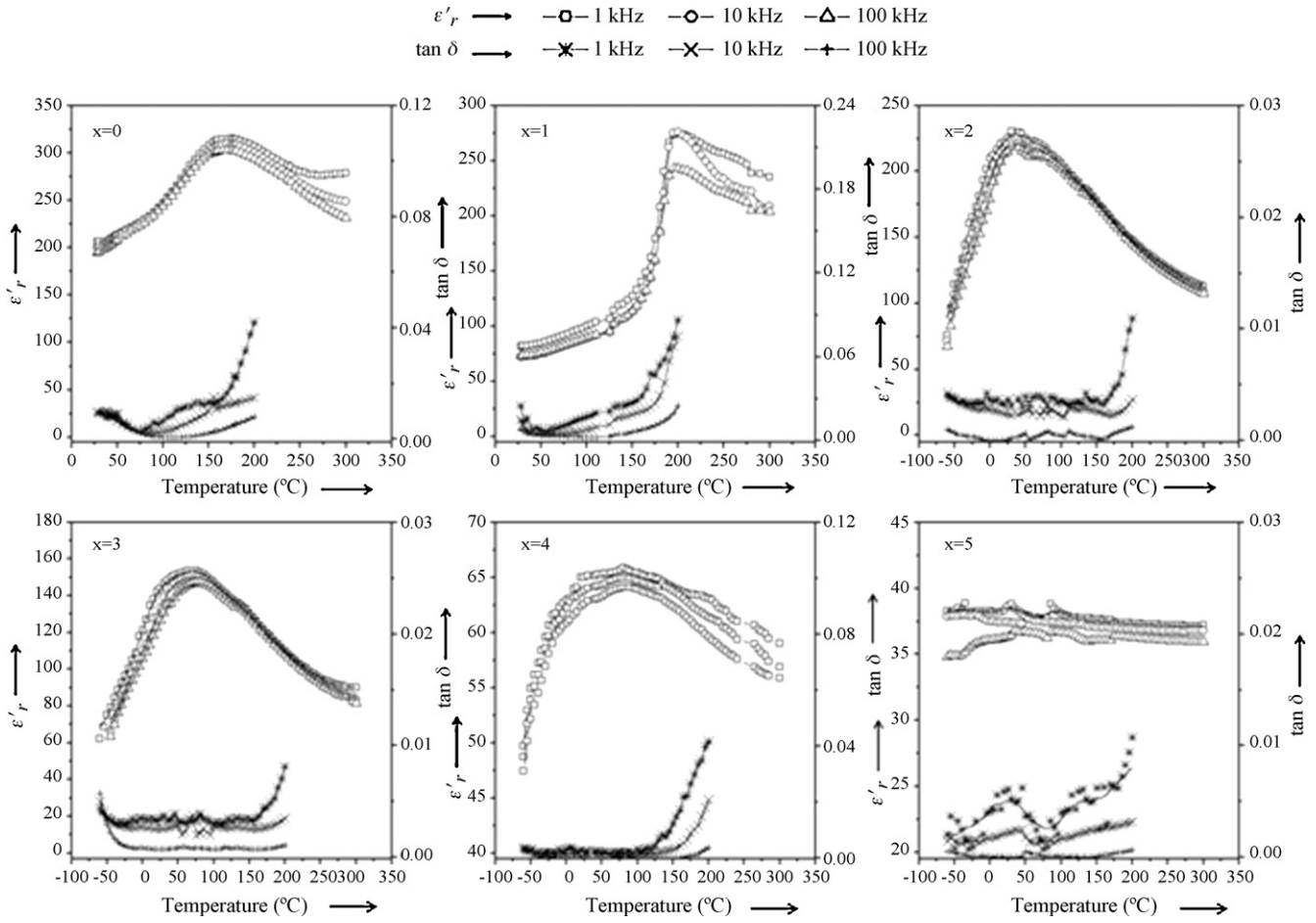

Fig. 4. Variation of dielectric constant (ε'_r) and dielectric loss ($\tan\delta$) with temperature at 1, 10 and 100 kHz frequencies of $(Ba_{1-x}Ca_x)_5SmTi_3Nb_7O_{30}$ compounds.

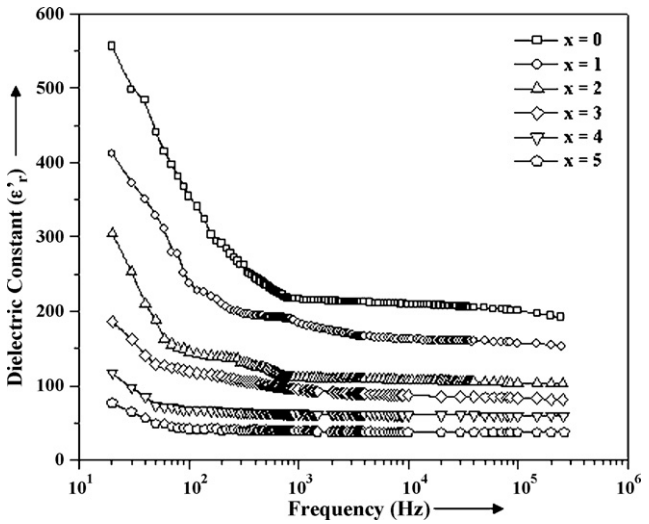

Fig. 5. Variation of dielectric constant (ε'_r) with frequency at room temperature.

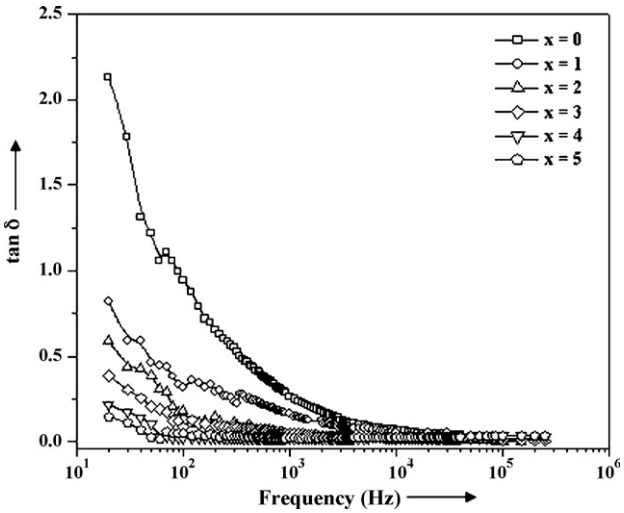

Fig. 6. Variation of dielectric loss ($\tan\delta$) with frequency at room temperature.

in calcium ($x = 1$) containing specimen. Larger value of tetragonal strain (c/a) on adding Ca (Fig. 2) indicates that a larger amount of thermal energy is required for the phase transition resulting in an increase in T_c. Another possible reason for the increase in the transition temperature could be attributed to the reduced value of the tolerance factor due to the partial substitution of smaller cation Ca at Ba-site [16]. However, for higher concentration of calcium (i.e., $x \geq 2$), T_c decreases sharply (Table 1). This is likely due to the formation of the secondary phase at these concentrations. At all the frequencies, the dielectric peak is found to be broadened indicating the existence of diffuse phase transition. The diffusivity constant (γ) have been calculated using the empirical relation [20]:

$$\ln\left(\frac{1}{\varepsilon'_r} - \frac{1}{\varepsilon'_{r\,\max}}\right) = \gamma \ln(T - T_c) + \text{constant} \quad (1)$$

where $\varepsilon'_{r\,\max}$ is the maximum ε'_r value at $T = T_c$. The value of γ at 100 kHz for all the samples are obtained from the slope of $\ln((1/\varepsilon'_r) - (1/\varepsilon'_{r\,\max}))$ versus $\ln(T - T_c)$ curve and are listed in Table 1. For all the studied compositions, γ is found to be between 1 (obeying Curie–Weiss law) and 2 (for completely disordered sys-

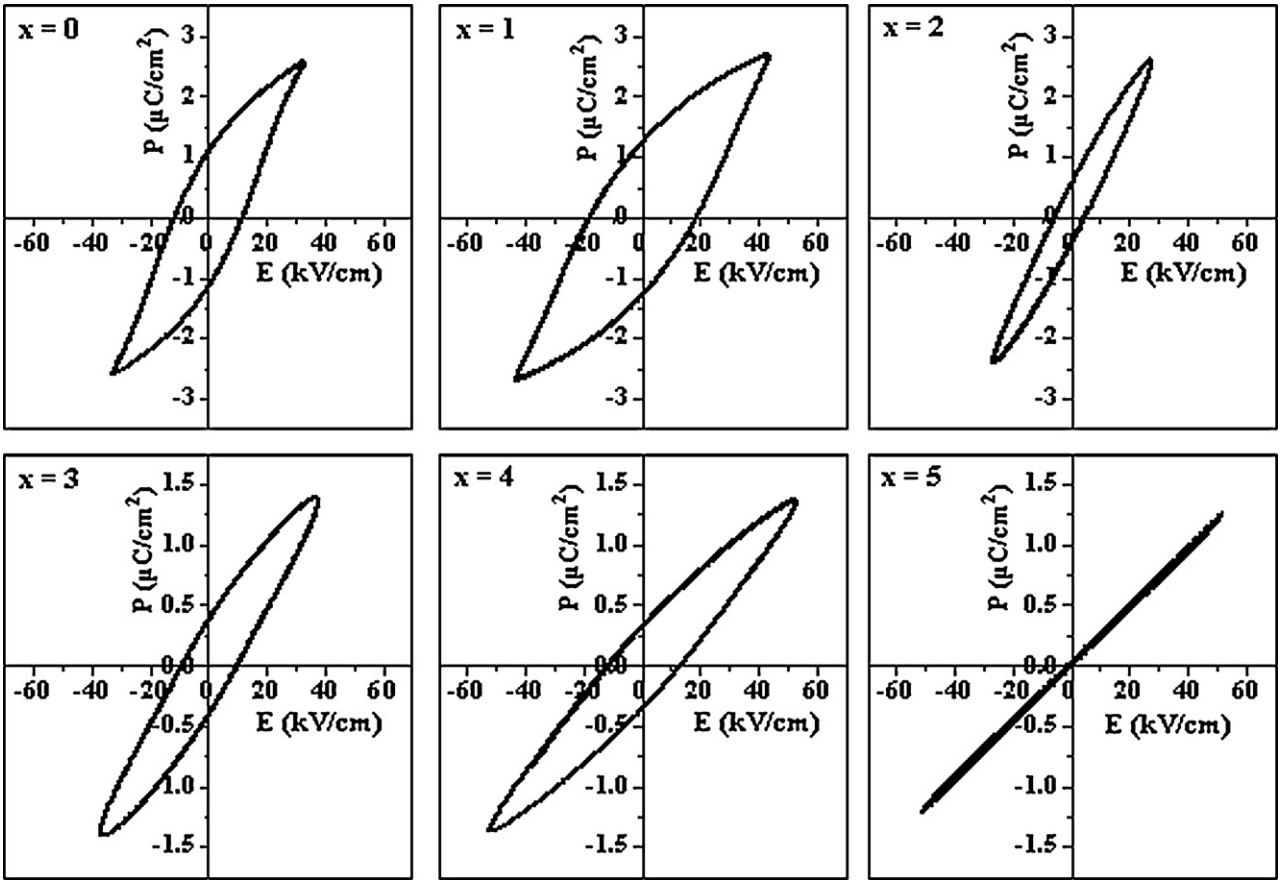

Fig. 7. *P–E* hysteresis loops of $Ba_{5-x}Ca_xSmTi_3Nb_7O_{30}$ ($x = 0$–5) compounds at room temperature.

tem) confirming the diffuse phase transition in all the samples. The value of γ is found to decrease from Ca free to $x = 1$ compound but it increases as concentration of calcium is further increased. It suggests that the composition with $x = 1$ is more ordered than other compositions [21]. For all the BCSTN compounds, at the above mentioned frequencies, the variation of dielectric loss with temperature (Fig. 4) shows that the loss is almost constant initially but at higher temperatures it increases sharply. This sharp increase of dielectric loss in high temperature region may be attributed to the increased mobility of space charges arising from the defects or vacancies (like oxygen vacancies) in the sample [22].

Fig. 5 shows the variation of dielectric constant with frequency from 20 Hz to 500 kHz at room temperature for all the compounds. For all the compositions, the dielectric constant decreases up to about 1 kHz and remains nearly constant beyond this frequency. The dielectric constant of a material has four polarization contributions: electronic, ionic, dipolar and space charge [23]. Response frequencies for ionic and electronic polarizations are $\sim 10^{13}$ and 10^{16} Hz, respectively; and at frequencies beyond 1 kHz, contribution from space charge polarization is not expected [23]. Thus, the higher values of dielectric constant at lower frequencies can be attributed to the presence of space charges in the structure which exist as defects such as oxygen vacancies [24,25]. Moreover, at lower frequencies, the dipoles can follow the alternating field resulting in higher values of dielectric constant while at higher frequencies the dipoles are unable to follow the rapidly changing field leading to the reduction in the values of dielectric constant.

The variation of dielectric loss with frequency at room temperature for all the compounds is shown in Fig. 6. It also decreases sharply up to 1 kHz and beyond this it is nearly independent of frequency. As discussed above, this can also be understood as the unability of the dipoles to follow the rapidly oscillating field at higher frequencies leading to the reduction in the values of dielectric loss. It can also be seen from Figs. 5 and 6 that the dielectric constant and dielectric loss at room temperature decreases with increase in calcium concentration.

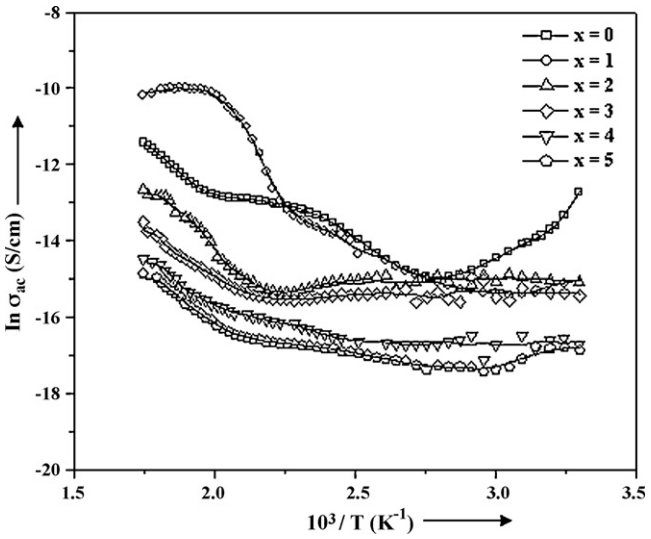

Fig. 9. Variation of ac conductivity ($\ln \sigma_{ac}$) with inverse of temperature ($10^3/T$) at 100 kHz frequency of $(Ba_{1-x}Ca_x)_5SmTi_3Nb_7O_{30}$ compounds.

3.3. Ferroelectric studies

To confirm the ferroelectric nature of the studied compounds, hysteresis loops were recorded at room temperature at a frequency of 100 Hz. Fig. 7 shows the variation of polarization as a function of electric field for all the compounds. The observed values

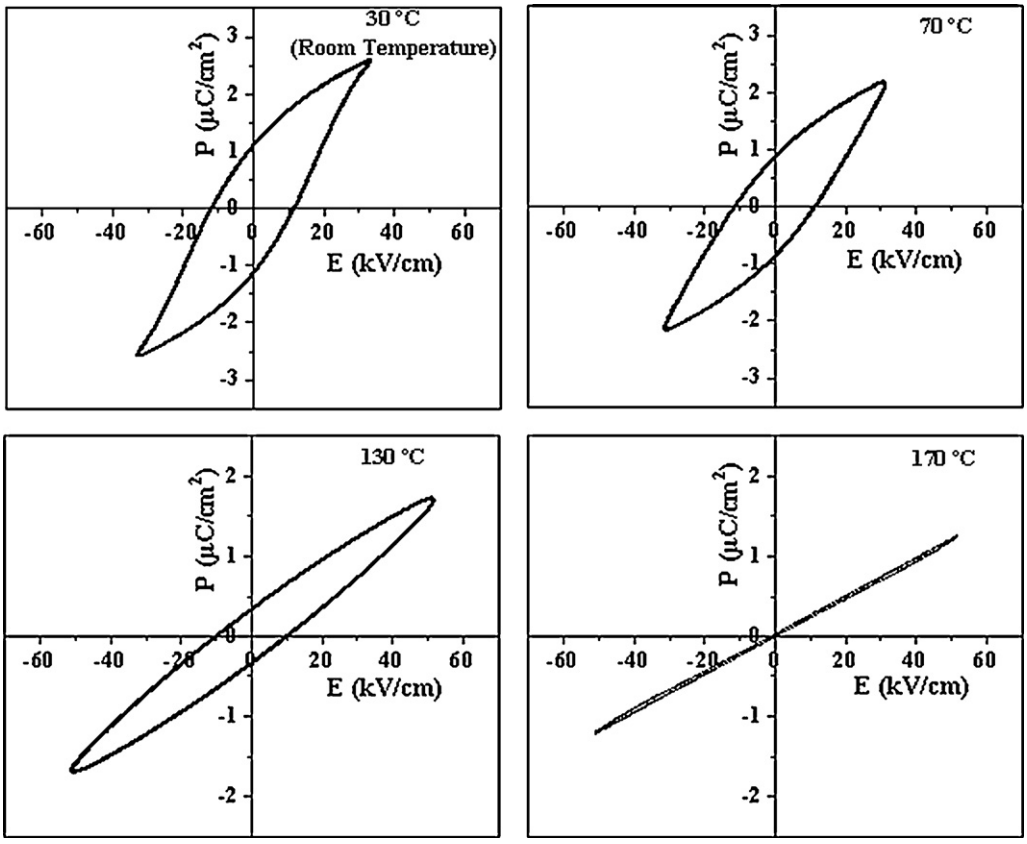

Fig. 8. Temperature variation of *P–E* hysteresis loop in $x = 0$ (i.e., $Ba_5SmTi_3Nb_7O_{30}$) compound.

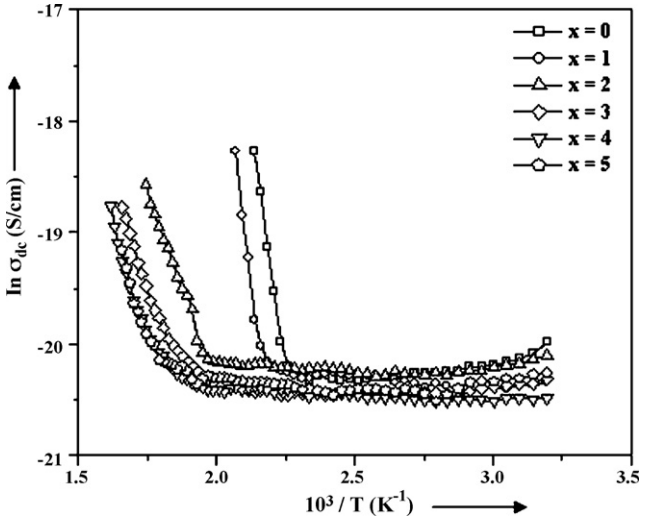

Fig. 10. Variation of dc conductivity ($\ln \sigma_{dc}$) with inverse of temperature ($10^3/T$) of $(Ba_{1-x}Ca_x)_5SmTi_3Nb_7O_{30}$ compounds.

of remanent polarization ($2P_r$) and the coercive field ($2E_c$) for all the compounds are given in Table 1. The remanent polarization ($2P_r$) is found to increase on Ca substitution, i.e., for the specimen with $x = 1$. The increase in remanent polarization could be correlated to the pronounced structural distortion arising due to the partial substitution of smaller cation Ca at Ba-site [16]. But for higher concentration of calcium, $2P_r$ decreases and finally the loop becomes a straight line for $x = 5$ confirming that the compound is no longer ferroelectric on completely replacing barium by calcium, which is in conformity with dielectric observations. The temperature variation of *P–E* hysteresis loop for $x = 0$ (i.e., $Ba_5SmTi_3Nb_7O_{30}$) specimen is shown in Fig. 8. It can be seen that the remanent polarization ($2P_r$) value decreases with increasing temperature and finally it becomes zero at the transition temperature (T_c), i.e., 170 °C.

3.4. AC and DC conductivity

The total conductivity (σ_{tot}) of the material comprises the ac conductivity (σ_{ac}) and the dc conductivity (σ_{dc}):

$$\sigma_{tot} = \sigma_{ac}(\omega) + \sigma_{dc} \quad (2)$$

The ac conductivity (σ_{ac}) and activation energy (E_a) of the sample have been calculated using the relation [26]:

$$\sigma_{ac} = \omega \varepsilon_r' \varepsilon_o \tan\delta = \sigma_o \exp\left(\frac{-E_a}{k_B T}\right) \quad (3)$$

where ω is the angular frequency, ε_o the free space permittivity and k_B the Boltzmann constant. The variation of ac conductivity as a function of inverse of temperature ($10^3/T$) for all the compositions at 100 kHz is shown in Fig. 9 and the calculated values of E_a of the samples are given in Table 1. The conductivity of the compounds at higher temperature is higher, which is a common behaviour in most of the dielectric ceramics [27,28]. The nature of variation of σ_{ac} over a wide temperature range supports the thermally activated conduction process in these materials. This is due to the presence of defects like oxygen vacancies whose mobility increases at higher temperatures [22].

Fig. 10 shows the variation of dc conductivity ($\sigma_{dc} = 1/\rho$) with inverse of temperature ($10^3/T$) for all the compositions. It can be seen from the figure that at low temperatures the conductivity is constant. But at higher temperatures, it increases with temperature indicating negative temperature coefficient of resistance (NTCR)-type behaviour in all the studied BCSTN compounds.

4. Conclusion

X-ray diffractograms confirm the formation of orthorhombic TB-structure in all the BCSTN compounds with decrease in orthorhombicity and increase in tetragonality on increasing the calcium concentration. Single phase is maintained for $x = 1$ beyond which increasing presence of $Ca_3Nb_2Ti_3O_{14}$ as secondary phase is indicated by XRD studies. Microstructural studies reveal that there is an increase in average grain size on substitution of calcium. The dielectric studies show that the value of dielectric constant decreases on addition of calcium. The Curie temperature (T_c), however, increases from 170 °C (for $x = 0$) to 198 °C (for $x = 1$). All the compounds exhibit non-relaxor type ferroelectric–paraelectric diffuse phase transition with least diffusivity in $x = 1$ composition except $x = 5$ where the compound does not show any phase transition. Negative temperature coefficient of resistance (NTCR) behaviour is being observed in all the compounds.

Acknowledgments

One of the authors (PG) is grateful to Council of Scientific and Industrial Research (CSIR), New Delhi, India for the award of Senior Research Fellowship.

References

[1] B. Wul, Nature 157 (1946) 808.
[2] N.S. Vandamme, A.E. Sutherland, L. Jones, K. Bridger, S.R. Winzer, J. Am. Ceram. Soc. 74 (1991) 1785–1792.
[3] R.R. Neurgaonkar, W.F. Hall, J.R. Oliver, W.W. Ho, W.K. Cory, Ferroelectrics 87 (1998) 167–179.
[4] R.R. Neurgaonkar, W.K. Cory, J. Opt. Soc. Am. B 3 (1986) 274–282.
[5] D. Liu, Y. Liu, S.Q. Huang, X. Yao, J. Am. Ceram. Soc. 76 (1993) 2129–2132.
[6] A. Panigrahi, N.K. Singh, R.N.P. Choudhary, J. Mater. Sci. Lett. 18 (1999) 1579–1581.
[7] P.B. Jasmieson, S.C. Abrahams, J.L. Bernstein, J. Chem. Phys. 48 (1965) 5048–5057.
[8] S.R. Shannigrahi, R.N.P. Choudhary, A. Kumar, H.N. Acharya, J. Phys. Chem. Solids 59 (1998) 737–742.
[9] P. Ganguly, A.K. Jha, K.L. Deori, J. Alloys Compd. 484 (2009) 40–44.
[10] R. Palai, R.N.P. Choudhary, H.S. Tewari, J. Phys. Chem. Solids 62 (2001) 695–700.
[11] P.R. Rao, S.K. Ghosh, P. Koshy, J. Mater. Sci.: Mater. Electron. 12 (2001) 729–732.
[12] J.L. Mukherjee, C.P. Khattak, K.P. Gupta, F.F.Y. Wang, J. Solid State Chem. 24 (1978) 163–167.
[13] P. Ganguly, A.K. Jha, K.L. Deori, J. Electroceram. 22 (2009) 257–262.
[14] C. Dong, J. Appl. Cryst. 32 (1999) 838.
[15] R.D. Shannon, C.T. Prewitt, Acta Crystogr. B 25 (1969) 925–946.
[16] R.R. Das, P. Bhattacharya, W. Perez, R.S. Katiyar, Ceram. Int. 30 (2004) 1175–1179.
[17] X.H. Zheng, X.M. Chen, Solid State Commun. 125 (2003) 449–454.
[18] L. Zhang, X.M. Chen, Solid State Commun. 149 (2009) 1317–1321.
[19] R.D. Shannon, J. Appl. Phys. 73 (1993) 348–366.
[20] S.M. Pilgrim, A.E. Sutherland, S.R. Winzer, J. Am. Ceram. Soc. 73 (1990) 3122–3125.
[21] T. Badapanda, S.K. Rout, S. Panigrahi, T.P. Sinha, Curr. Appl. Phys. 9 (2009) 727–731.
[22] T. Friessnegg, S. Aggarwal, R. Ramesh, B. Nielsen, E.H. Poindexter, D.J. Keeble, Appl. Phys. Lett. 77 (2000) 127–129.
[23] R.C. Buchanan, Ceramic Materials for Electronics: Processing, Properties and Applications, Marcel Dekker, Inc., New York, 1991.
[24] Y. Noguchi, M. Miyayama, Appl. Phys. Lett. 78 (2001) 1903–1905.
[25] A. Chen, Y. Zhi, L.E. Cross, Phys. Rev. B 62 (2000) 228–236.
[26] W.D. Kingery, Introduction to Ceramics, Wiley, New York, 1960.
[27] K.S. Singh, R. Sati, R.N.P. Choudhary, Pramana 38 (1992) 161–166.
[28] K.S. Rao, T.N.V.K.V. Prasad, A.S.V. Subrahmanyam, J.H. Lee, J.J. Kim, S.H. Cho, Mater. Sci. Eng. B 98 (2003) 279–285.